

# ON SETTING A PRESSURE DATUM WHEN COMPUTING INCOMPRESSIBLE FLOWS

ANDREW YECKEL AND JEFFREY J. DERBY\*

*Department of Chemical Engineering and Materials Science, Army High Performance Computing Research Center,  
University of Minnesota, Minneapolis, MN 55455-0132, USA*

## SUMMARY

The conventional approach to set the pressure level in a finite element discretization of an enclosed, steady, incompressible flow is to discard a continuity residual and set the associated pressure basis function coefficient to a desired value. Two issues surrounding this setting of a pressure datum are explored. First, it is shown that setting a boundary traction at a single node, in lieu of a Dirichlet velocity condition, is a preferred alternative for use with pressure-stabilized finite element methods. Second, it is shown that setting a pressure datum can slow or even stop the convergence of a GMRES-based iterative solver; though by some appearances a solution may appear to be converged, significant local errors in the velocity may exist. Under such circumstances it is preferable to solve the consistent singular system of equations, rather than setting a pressure datum. It is shown that GMRES converges in such cases, implicitly setting a pressure level that is determined from the initial guess. Copyright © 1999 John Wiley & Sons, Ltd.

## 1. BACKGROUND

There has been a long history of research on proper and useful representations of the pressure field in finite element computations of incompressible flows. This prior research has resulted in conventional approaches involving mixed-order interpolation with the Galerkin finite element method (GFEM) and newer approaches employing equal-order interpolation with stabilized methods. Irrespective of the approach employed for computation, the solution of an incompressible flow within an enclosed domain contains a hydrostatic pressure mode that causes the pressure field to be indeterminate with respect to an arbitrary constant. Accommodating this simple effect is straightforward when employing classical GFEM techniques in conjunction with direct solution methods, but some important issues associated with the hydrostatic pressure mode when using newer finite element implementations, and when using iterative solution methods are discussed below.

The relationship between the hydrostatic pressure mode and mass continuity of an incompressible fluid was clearly elucidated by Sani *et al.* [1,2] and Engelman *et al.* [3]. Following their work, our starting point is the statement of global mass conservation

$$\int_{\Omega} \nabla \cdot \mathbf{u} \, d\Omega = 0, \quad (1)$$

\* Correspondence to: Department of Chemical Engineering and Materials Science, University of Minnesota, Minneapolis, MN 55455-0132, USA. Fax: +1 612 6267246; e-mail: derby@maroon.tc.umn.edu

where  $\Omega$  constitutes the entire domain. By application of the divergence theorem, Equation (1) is transformed to an equivalent condition:

$$\int_{\Gamma} \mathbf{n} \cdot \mathbf{u} \, d\Gamma = 0, \quad (2)$$

where  $\Gamma$  constitutes the entire boundary of the domain.

As shown in Sani *et al.* [1], the weak form of the equations used in the Galerkin finite element method enforces the condition prescribed by Equation (1), with the finite element approximation to the velocity field substituted for the exact velocity field. Furthermore, if the normal velocity is specified at all boundaries (either pointwise or in an integral sense) as is the case for all enclosed flows, then Equation (2) must be satisfied exactly, otherwise the problem is ill-posed and no solution exists. Engelman *et al.* [3] describe the use of mass-consistent normals to ensure that the boundary data satisfy Equation (2) exactly. While mass consistency averts the situation of an ill-posed problem, the matrix that results from the discretization has a rank one deficiency because of the hydrostatic pressure mode, and therefore is singular. This situation is subsequently referred to as the consistent singular formulation (throughout this work it is assumed that the hydrostatic pressure mode is the only cause of singularity; bifurcation points are not treated, nor are the spurious pressure modes that arise with certain pressure and velocity basis function combinations).

This singularity in the discrete equations does not always lead to problems. Engelman *et al.* [3] pointed out that, provided the boundary conditions satisfy Equation (2) to machine precision, the finite arithmetic of the computer dictates that the following equation will be encountered during Gaussian elimination:

$$\epsilon_1 p = \epsilon_2, \quad (3)$$

where  $\epsilon_i$  is an  $\mathcal{O}(1)$  random number multiplied by the round-off level of the computer, and  $p$  is a pressure unknown. Thus, an  $\mathcal{O}(1)$  random value is obtained for  $p$ , thereby setting a reasonable, but arbitrary, pressure datum.

An alternate approach for dealing with the rank one deficiency, widely used because of the convenience of its application, is to discard a single continuity residual that is readily identified with a specific pressure value within the problem domain. The pressure basis function coefficient associated with that residual is set to a chosen level, e.g. zero. This approach is commonly described as setting a pressure datum. By discarding a single continuity residual, the condition of global mass conservation stated in Equation (1) is relaxed. Global mass conservation is still assured to the extent that Equation (2) is satisfied by the boundary data. If this is not the case, a non-zero divergence occurs within the domain, generally isolated to the immediate neighborhood of the element at which the pressure datum is set, but the problem remains well-posed.

Setting a pressure datum is not always a suitable approach, however. In particular, discarding a single residual violates the completeness of stabilized finite element formulations, such as PSPG (pressure-stabilized Petrov–Galerkin) [4,5] and GLS (Galerkin least squares) [5,6], since the weighted residuals of these methods blend components of the continuity and momentum equations together. An alternate approach suitable to these formulations is described and tested in Section 3.1 of this paper. An approach similar to the ‘node-freeing’ idea put forth by Sani *et al.* [2] is employed, whereby the normal component of the traction is set at a single node, thereby establishing the global pressure level. This procedure requires that a single momentum residual be retained at the boundary, in lieu of applying a boundary condition on the normal velocity at that point. Doing so relaxes the condition of global mass

conservation given by Equation (2). Global mass conservation is assured, however, because Equation (1) is still satisfied by the pressure-stabilized formulation.

Another circumstance in which setting a pressure datum can be problematic is when using an iterative solver on the linear system of equations that arises from the finite element discretization. Section 3.2 shows that imposing a pressure datum can greatly retard convergence of a GMRES-based iterative solver [7,8], particularly when solving large three-dimensional problems. When solution convergence is judged by conventional criteria, it may appear that the solution is converged, or very nearly converged, when in fact significant local errors in the velocity may exist. This phenomenon occurs when using either classical Galerkin or pressure-stabilized formulations. Substituting a boundary traction in the manner described in Section 3.1 does not ameliorate the problem. Fortunately, it proves unnecessary to set either a pressure datum or a boundary traction when using GMRES. Indeed, a recent work by Brown and Walker [9] proves that under certain conditions, GMRES and equivalent methods converge to a least-squares solution of singular linear systems. We show that the conditions laid out in Reference [9] apply in the case of the singular systems considered here. We also show that under such conditions GMRES implicitly determines a unique pressure level that is a function of the initial guess.

## 2. PROBLEM FORMULATION AND DISCRETIZATION

We consider flows governed by the steady Navier–Stokes equations, written in dimensionless form for an incompressible fluid, as

$$Re \mathbf{u} \cdot \nabla \mathbf{u} = \nabla \cdot \mathbf{T}, \quad (4)$$

$$\nabla \cdot \mathbf{u} = 0, \quad (5)$$

where  $\mathbf{T} = -p\mathbf{I} + \nabla \mathbf{u} + (\nabla \mathbf{u})^T$  is the total stress tensor, and  $\mathbf{I}$  the identity tensor. The fluid velocity  $\mathbf{u}$  is measured in units of a characteristic velocity  $V$ , the dynamic pressure  $p$  in units of  $\mu V/L$ , and Cartesian co-ordinates  $x$ ,  $y$  and  $z$  in units of  $L$ , where  $L$  is a characteristic length and  $\mu$  is the fluid viscosity. The effect of inertia is characterized by the Reynolds number,  $Re = \rho V L / \mu$ , where  $\rho$  is the fluid density. Boundary conditions on the various problems solved are described elsewhere in this paper.

Several finite element discretizations of Equations (4) and (5) are used in this paper. In Section 3.1, two-dimensional problems are discretized using both the GFEM (Galerkin finite element method) with biquadratic velocity–linear-discontinuous pressure elements [10] and the PSPG (pressure-stabilized Petrov–Galerkin) formulation with bilinear velocity–bilinear pressure elements [4,5]. In both cases a structured mesh of quadrilaterals is used. In Section 3.2, three-dimensional problems are discretized using the GFEM with triquadratic velocity–linear-discontinuous pressure elements over a structured mesh of hexahedra.

In all cases, standard procedures are applied to obtain weak-form weighted residuals, denoted as

$$\mathbf{R}(\mathbf{y}) = 0, \quad (6)$$

where  $\mathbf{R}$  is a non-linear vector equation and  $\mathbf{y}$  is the vector of velocity and pressure basis function coefficients. Equation (6) is solved using the Newton iteration. An initial guess of the vector of unknowns is made,  $\mathbf{y}^{(0)}$ , and successive updates to the unknowns vector are computed using

$$\mathbf{y}^{(k+1)} = \mathbf{y}^{(k)} + \mathbf{x}^{(k)}, \quad (7)$$

where  $k$  is the iteration counter. The update vector  $\mathbf{x}^{(k)}$  is generated by solution of the linear equation set

$$\mathbf{J}(\mathbf{y}^{(k)})\mathbf{x}^{(k)} = -\mathbf{R}(\mathbf{y}^{(k)}), \quad (8)$$

where  $J_{ij} = \partial R_i / \partial y_j$  are elements of the Jacobian matrix. Equation (8) is solved using a direct frontal routine in the two-dimensional problems and the GMRES (generalized minimal residual) iterative method of Saad and Schultz [7,8] in the three-dimensional problems. GMRES is used with diagonal preconditioning and restarting, as described in Yeckel and Derby [11].

To terminate the Newton iteration it is necessary to judge when the solution to the residuals is converged. Treating the solution update as a continuous function (the update vector is interpolated using the basis functions), two norms are computed, the  $L_2$ -norm and the  $L_\infty$ -norm:

$$L_{2,\text{update}} = \|\mathbf{x}\|_2 = \left\{ \int_{\Omega} (|\delta u|^2 + |\delta v|^2 + |\delta w|^2 + |\delta p|^2) dA \right\}^{1/2} \approx \left\{ \frac{1}{N} \sum_{i=1}^N x_i^2 \right\}^{1/2}, \quad (9)$$

$$L_{\infty,\text{update}} = \|\mathbf{x}\|_{\infty} = \max_{\Omega} (|\delta u|, |\delta v|, |\delta w|, |\delta p|) \approx \max_i |x_i|, \quad (10)$$

where  $\delta u$ ,  $\delta v$ ,  $\delta w$ , and  $\delta p$  are the update fields of the velocity components and pressure. Equation (9) approximates a spatial average of the update, therefore, it is a more useful criterion than the widely used  $L_2$  vector-norm, the interpretation of which depends on the problem size  $N$ . Similar norms are also computed for the residual Equation (6):

$$L_{2,\text{residual}} = \|\mathbf{R}\|_2 \approx \left\{ \frac{1}{N} \sum_{i=1}^N R_i^2 \right\}^{1/2}, \quad (11)$$

$$L_{\infty,\text{residual}} = \|\mathbf{R}\|_{\infty} \approx \max_i |R_i|. \quad (12)$$

The issue of determining suitable tolerances for these norms for assessing whether a solution is adequately converged is discussed later.

The two-dimensional problems of Section 3.1 are solved using a serial workstation (a PowerComputing Power 120), and the three-dimensional problems of Section 3.2 are solved using the Thinking Machines Corporation CM-5, a distributed memory, multi-processor supercomputer. Interested readers should consult Reference [12] for more details on the parallel implementation of the algorithms used to solve the three-dimensional problems.

### 3. RESULTS AND DISCUSSION

#### 3.1. Setting the pressure level when using stabilized methods

Stabilized finite element methods differ from the GFEM in that individual residuals can no longer be identified entirely with momentum or continuity. Instead, the residuals all represent some linear combination of momentum and continuity contributions. Residuals can be identified with the basis function type that weights them, however. For example, the GLS and PSPG residuals weighted by the pressure basis functions  $\psi_i$  take the form

$$\int_{\Omega} \psi_i \nabla \cdot \mathbf{u}^h d\Omega + \sum_{e=1}^{N_{el}} \int_{\Omega^e} \tau \nabla \psi_i \cdot [Re\mathbf{u}^h \cdot \nabla \mathbf{u}^h - \nabla \cdot \mathbf{T}^h] d\Omega = 0, \quad (13)$$

where  $\mathbf{T}^h$  is the total stress tensor computed using  $\mathbf{u}^h$  and  $p^h$ , the finite element approximations to the velocity and pressure. These are approximated in terms of piecewise polynomial basis functions  $\phi$  and  $\psi$ , as

$$\mathbf{u}^h = \sum_{k=1}^N \mathbf{u}_k \phi_k(\mathbf{x}), \quad (14)$$

$$p^h = \sum_{k=1}^M p_k \psi_k(\mathbf{x}). \quad (15)$$

Note that the first integral in Equation (13) corresponds to the continuity residuals in the GFEM. In PSPG and GLS these residuals are modified by the stabilizing term given in the second integral. The parameter  $\tau$  is obtained by non-dimensionalizing the definition given in Reference [5].

Gresho, Sani, and co-workers have shown that it is of paramount importance that any finite element formulation satisfies global mass conservation [1–3,13,14]. Following their work, and noting

$$\sum_{i=1}^{M_h} \psi_i = 1, \quad \sum_{i=1}^{M_h} \nabla \psi_i = 0, \quad (16)$$

it is clear that a summation of Equation (13) over the appropriate subset of  $M_h$  pressure basis functions enforces global mass conservation. Because the space of pressure basis functions must always contain the hydrostatic pressure level, Equation (16) must be satisfied by some subset  $M_h$  of any valid basis function set.

In principle, the second term of Equation (13) could be zero, assuming an exact solution to Equations (4) and (5) could be represented by  $\mathbf{u}^h$ . In practice, however, this cannot be the case in a non-trivial flow. A non-zero contribution is required to achieve stabilization of element types that use equal-order interpolation for velocity and pressure. Therefore, the validity of discarding one of these residuals in order to set a pressure basis coefficient is subject to question, because doing so implies that the second term is identically zero over the element in question. This supposition violates the least-squares minimization procedure, at least locally, when applied to the GLS formulation. On the other hand, this second term should be small, so a large error is not expected to be induced by this procedure. To be certain, however, we seek an alternative that allows us to remove the redundant specification of global mass conservation that occurs when the boundary data imply Equation (2), while at the same time establishing the pressure level.

As noted previously, Sani *et al.* [2] put forth an alternative to setting a pressure datum, which they refer to as ‘node freeing’. They applied the node-freeing idea in the context of the non-physical checkerboard pressure mode. This mode is caused by a redundant constraint among the tangential boundary velocities that arises when certain combinations of boundary conditions and basis function types are used. The mode can be eliminated by relaxing one of the redundant constraints. Setting a pressure datum is one way to do so. Another way is the node-freeing alternative, in which a tangential boundary traction is set at a single node, thereby retaining a single momentum residual at the boundary. A similar approach, described here, can be applied to eliminate the hydrostatic mode.

The key to eliminating the hydrostatic pressure mode is to eliminate the redundancy of Equations (1) and (2). In setting a pressure datum, this task is accomplished by discarding one of the continuity residuals, which has the effect of removing Equation (1) from the equation set. The node-freeing method proposed here is to remove Equation (2) from the equation set.

The procedure is based on imposing the normal component of traction at a single node along the boundary in lieu of imposing a condition on the normal component of velocity there. How this is done depends on how the boundary data are enforced and is best illustrated via examples.

In the simplest case, Dirichlet boundary conditions are imposed by specifying values of all velocity components along the boundary (it is assumed that the specified values are consistent with Equation (2)). Ordinarily, all momentum residuals at those nodes are discarded from the equation set. Should the normal to a boundary lie in the direction of a co-ordinates axis, the node-freeing procedure is to retain a *single residual* that represents the normal component of momentum associated with one of the boundary nodes. It follows that the value of the normal velocity component at that node is not specified, but must be computed as part of the solution. If, e.g.  $x$  is constant along some boundary, then the  $x$ -momentum residual is retained in lieu of specifying the value of the  $u$  component of velocity. Of course, since Equation (1) is satisfied by any solution to the equations, the computed value of the normal component of velocity must be consistent with global mass conservation, therefore it must equal zero.

In addition to eliminating the redundancy of Equations (1) and (2), the node-freeing procedure must also set the global pressure level. To do so properly requires use of the stress-divergence form of the momentum equations. Then applying the natural boundary condition on the momentum residual at the boundary node amounts to specifying the normal traction, which effectively determines the global pressure level (see, e.g. Reference [14]). Since the pressure level is arbitrary, it is convenient to impose no boundary condition at all, which is equivalent to a normal traction equal to zero.

The situation is slightly more complicated when the boundary normal does not lie conveniently in the direction of a co-ordinate axis. In the two-dimensional case it is necessary to replace Dirichlet conditions on  $u$  and  $v$  at a *single* boundary node with the conditions

$$\mathbf{t} \cdot \mathbf{u} = V_t, \quad (17)$$

$$\mathbf{n} \cdot \mathbf{M} = n_x M_x + n_y M_y = 0, \quad (18)$$

where  $V_t$  is the specified value of the tangential velocity,  $M_x$  and  $M_y$  are the  $x$ - and  $y$ -momentum residuals, and  $\mathbf{n}$  and  $\mathbf{t}$  are the unit normal and tangent at the boundary. In three dimensions it is necessary to add an additional condition on the tangential component of the velocity to replace the Dirichlet condition on  $w$ . If the boundary is curved, it may be necessary to use the method of mass-consistent normals of Engelman *et al.* [3] to obtain a computed normal velocity component equal to zero at the affected node, but in principal, the node-freeing procedure is the same.

Clearly, it possible to use node-freeing as a substitute for setting a pressure datum, irrespective of the conditions imposed on the tangential component of velocity or momentum, providing the boundary data are consistent with Equation (2). Hence the procedure can be more generally implemented than demonstrated by the case discussed above, in which Dirichlet conditions are used for all velocity components.

To validate the approach just described, we solve for a  $Re = 10$  flow in a lid-driven cavity on a unit square, using both GFEM and PSPG formulations. No-slip boundary conditions are imposed at all boundaries, and one side of the cavity translates at uniform speed. A direct frontal routine is employed to solve the linear system (8). Uniform meshes of  $20 \times 20$  elements (GFEM case) and  $40 \times 40$  elements (PSPG case) are used, which results in discretizations of roughly equal number of unknowns. Tables I and II show results of the GFEM and PSPG cases, respectively. Characteristic solution quantities given in the table include  $\psi_{\min}$ , the

Table I. GFEM-discretized 2D lid-driven cavity results (symbols explained in text)

Formulation	$\psi_{\min}$	$\Delta p_{\max}$	$\int_{\Omega} \nabla \cdot \mathbf{u}^h d\Omega$	$V_n$
Consistent singular	$-9.9964 \times 10^{-2}$	295.8	$9 \times 10^{-13}$	–
Pressure datum	$-9.9964 \times 10^{-2}$	295.8	$-8 \times 10^{-13}$	–
Traction (U-lower left)	$-9.9964 \times 10^{-2}$	295.8	$-6 \times 10^{-13}$	$-8 \times 10^{-14}$
Traction (V-lower left)	$-9.9964 \times 10^{-2}$	295.8	$-6 \times 10^{-13}$	$-8 \times 10^{-14}$
Traction (V-upper left)	$-9.9964 \times 10^{-2}$	295.8	$-6 \times 10^{-13}$	$8 \times 10^{-14}$
Traction (U-upper left)	$-9.9964 \times 10^{-2}$	295.8	$-6 \times 10^{-13}$	$-8 \times 10^{-14}$

streamfunction value at the center of the primary vortex;  $\Delta p_{\max}$ , the maximum pressure difference over the entire cavity; the global divergence  $\int_{\Omega} \nabla \cdot \mathbf{u}^h d\Omega$ ; and  $V_n$ , the normal velocity component at the node where the normal traction is set to zero.

The agreement between the two computed solutions is excellent. The value of  $\psi_{\min}$  computed using the PSPG formulation agrees to within 0.2% of the value computed using the GFEM. This small discrepancy might be explained by our neglecting the stabilization terms arising from the deviatoric terms of the stress tensor in Equation (13). It should be noted that the large difference in  $\Delta p_{\max}$  between the two formulations is no cause for concern. There are non-integrable singularities in the continuum statement of the lid-driven cavity problem, therefore, the maximum and minimum pressures grow without bound as the mesh is refined. Thus,  $\Delta p_{\max}$  is merely useful when comparing solutions obtained on the same mesh with the same basis functions.

The GFEM results shown in Table I corroborate the new approach against the more conventional technique of setting a pressure datum directly. First, note that setting a pressure datum yields essentially the same results as obtained from the consistent singular formulation (i.e. the approach of doing nothing). The only difference in the solution is a different absolute pressure level. Note also that because the lid-driven cavity has straight sides, mass-consistency is achieved without employing mass-consistent normals. The new boundary traction approach (i.e. the node-freeing formulation) was tested at four different locations in the GFEM case, to assure that the correct velocity  $V_n$  is computed irrespective of the location. Indeed, the computed value of  $V_n$  is virtually zero, as it should be according to Equation (2).

The PSPG results are shown in Table II and are consistent with the GFEM results. Clearly, the boundary traction approach yields valid results that are identical to those obtained using the conventional pressure datum approach.

Table II. PSPG-discretized 2D lid-driven cavity results (symbols explained in text)

Formulation	$\psi_{\min}$	$\Delta p_{\max}$	$\int_{\Omega} \nabla \cdot \mathbf{u}^h d\Omega$	$V_n$
Consistent singular	$-9.9802 \times 10^{-2}$	406.4	$-1 \times 10^{-11}$	–
Pressure datum	$-9.9802 \times 10^{-2}$	406.4	$-1 \times 10^{-11}$	–
Traction	$-9.9802 \times 10^{-2}$	406.4	$-1 \times 10^{-11}$	$-5 \times 10^{-14}$

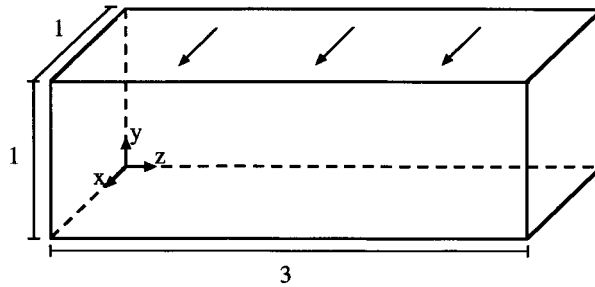


Figure 1. Domain of the three-dimensional lid-driven cavity.

### 3.2. Setting the pressure level when using GMRES

The results and discussion in this paper thus far have been predicated on the assumption that the linear system can be solved to a high degree of precision at each Newton iteration via a direct solver. However, it is not always possible to use a direct method when solving large three-dimensional problems, due to computer memory limitations or excessive operation counts. Therefore, an iterative method of some sort must be used to solve the linear system. Although it is theoretically possible to solve a linear system to a high degree of precision using an iterative solver, it is often not feasible for a number of reasons ranging from inadequate preconditioning to computer round-off error. Even in those cases where it is feasible, it may be unaffordable because of memory or operation count limitations.

Here we consider the implications of solving the consistent singular system using an iterative solver and the effect of setting a pressure datum on convergence. We confine ourselves to reporting our experience using GMRES [7,8], but speculate that the phenomenon reported here applies to other projection-based iterative solvers as well. The test problem is the three-dimensional lid-driven cavity [15–17]; the domain is shown in Figure 1. No-slip boundary conditions are applied everywhere. The top surface, exclusive of the edge nodes, moves at constant velocity in the direction indicated. A mesh of  $10 \times 10 \times 20$  elements (62243 unknowns) is used unless otherwise noted.

In GMRES, the linear system of equations (8) is projected onto a Krylov subspace. Then an approximate solution  $\mathbf{x}_m^{(k)}$  is computed, and minimizes the  $L_2$ -norm of the residuals of the linear system, given by

$$L_{2,\text{GMRES}} = \|\mathbf{J}\mathbf{x}_m^{(k)} + \mathbf{R}\|_2 = \sqrt{\sum_{i=1}^N (J_{ij}x_{m,j}^{(k)} + R_i)^2}, \quad (19)$$

where summation over  $j$  is implied. A solution that minimizes Equation (19) is referred to as a least-squares solution, provided that GMRES converges without breakdown. The subscript  $m$  refers to the  $m$ th GMRES iterate in the solution of Equation (8). To be of practical use, the Krylov subspace should be much smaller than the original system (typically we use a subspace size of 25–100 in problems with  $10^5$ – $10^6$  unknowns). Often such a small subspace cannot give a satisfactory approximation to  $\mathbf{x}_m^{(k)}$  without restarting, as described in Saad [8]. Even then the method can stagnate, which means that a point is reached where further restarting no longer reduces  $L_{2,\text{GMRES}}$  to a meaningful extent. Our approach, described in Reference [11], is to take the Newton step after a maximum number of restarts (typically 20) has been reached, or the

method has stagnated, regardless of the size of  $L_{2,\text{GMRES}}$ . Of course, enough Newton iterations are taken to assure convergence of the original problem.

The GMRES method does not strictly require that the linear system of equations is well-posed. Indeed, Brown and Walker [9] have recently shown that if the null space of  $\mathbf{J}$  is equivalent to the null space of  $\mathbf{J}^T$ , then GMRES converges without breakdown to a least-squares solution that minimizes Equation (19). It is assumed that the hydrostatic pressure mode is the only cause of singularity, therefore, the null space of  $\mathbf{J}$  consists solely of that mode. For any square matrix, the dimension of the null space of the transpose of a matrix is identical to the dimension of the null space of the matrix. Therefore it is sufficient to prove that the hydrostatic pressure mode belongs to the null space of  $\mathbf{J}^T$ , i.e. given  $\mathbf{J}\mathbf{h} = \mathbf{0}$ , then  $\mathbf{J}^T\mathbf{h} = \mathbf{0}$ , where  $\mathbf{h}$  is the hydrostatic null vector. To prove this, first we note that the GFEM discretization can be written in matrix form [1,18], as

$$[\mathbf{K} + \mathbf{N}(\mathbf{U})]\mathbf{U} + \mathbf{C}\mathbf{P} = \mathbf{f},$$

$$\mathbf{C}^T\mathbf{U} = \mathbf{g}, \quad (20)$$

where  $\mathbf{U}$  is a vector of velocity unknowns and  $\mathbf{P}$  is a vector of pressure unknowns. Also,  $\mathbf{K}$  is the viscous stress matrix,  $\mathbf{N}(\mathbf{U})$  is the advection matrix,  $\mathbf{C}$  is the pressure gradient matrix,  $\mathbf{C}^T$  is the divergence matrix, and  $\mathbf{f}$  and  $\mathbf{g}$  account for the effect of boundary conditions (see Reference [18] for a more detailed description of these terms). Observing that elements of  $\mathbf{h}$  corresponding to velocity unknowns are identically zero,  $\mathbf{J}\mathbf{h}$  takes the form

$$\mathbf{J}\mathbf{h} = \begin{bmatrix} [\mathbf{K} + \mathbf{N}(\mathbf{U}) + \mathbf{N}'(\mathbf{U})\mathbf{U}] & \mathbf{C} \\ \mathbf{C}^T & \mathbf{0} \end{bmatrix} \begin{bmatrix} 0 \\ \mathbf{h}_p \end{bmatrix} = \begin{bmatrix} \mathbf{C}\mathbf{h}_p \\ 0 \end{bmatrix} = \mathbf{0}, \quad (21)$$

from which it follows that  $\mathbf{C}\mathbf{h}_p = \mathbf{0}$ , a result previously obtained by Sani *et al.* [1]. Since  $(\mathbf{C}^T)^T = \mathbf{C}$ ,  $\mathbf{J}^T\mathbf{h}$  also implies that  $\mathbf{C}\mathbf{h}_p = \mathbf{0}$ . Thus  $\mathbf{h}$  belongs to the null space of  $\mathbf{J}^T$ , which completes the proof.

We note in passing that another pressure mode, the pure checkerboard mode, is also characterized by the condition that  $\mathbf{C}\mathbf{h}_p = \mathbf{0}$  [1]. Therefore, it is expected that GMRES will converge when this mode is present, either alone or in conjunction with the hydrostatic mode.

Pressure-stabilized methods such as PSPG and GLS do not produce the symmetry of the off-diagonal blocks given by the GFEM in Equation (21). In the PSPG method, for example,  $\mathbf{J}\mathbf{h}$  is given by

$$\mathbf{J}\mathbf{h} = \begin{bmatrix} [\mathbf{K} + \mathbf{N}(\mathbf{U}) + \mathbf{N}'(\mathbf{U})\mathbf{U}] & \mathbf{C} \\ \mathbf{C}^T + \mathbf{G}_v^T & \mathbf{G}_p \end{bmatrix} \begin{bmatrix} 0 \\ \mathbf{h}_p \end{bmatrix} = \begin{bmatrix} \mathbf{C}\mathbf{h}_p \\ \mathbf{G}_p\mathbf{h}_p \end{bmatrix} = \mathbf{0}, \quad (22)$$

where the additional contributions  $\mathbf{G}_v$  and  $\mathbf{G}_p$  correspond to the stabilizing terms in the second integral in Equation (13). Note that for  $\mathbf{h}$  to be the hydrostatic null vector requires that  $\mathbf{G}_p\mathbf{h}_p = \mathbf{0}$ , in addition to  $\mathbf{C}\mathbf{h}_p = \mathbf{0}$ . Also, to prove that  $\mathbf{J}^T\mathbf{h} = \mathbf{0}$  requires proving that  $\mathbf{G}_v\mathbf{h}_p = \mathbf{0}$  and  $\mathbf{G}_p^T\mathbf{h}_p = \mathbf{0}$ . From Equation (13) we obtain

$$G_{p,ij} = \sum_{e=1}^{N_{el}} \int_{\Omega^e} \tau \nabla\psi_i \cdot \nabla\psi_j \, d\Omega, \quad (23)$$

$$G_{v,ij}^T = \sum_{e=1}^{N_{el}} \int_{\Omega^e} \tau \nabla \psi_i \cdot \frac{\partial [Re\mathbf{u}^h \cdot \nabla \mathbf{u}^h - \nabla \cdot \mathbf{T}^h]}{\partial u_j} d\Omega, \quad (24)$$

where  $u_j$  refers to all velocity basis function coefficients. It follows that

$$(\mathbf{G}_p \mathbf{h}_p)_i = \sum_{j=1}^M G_{p,ij} h_{p,j} = \sum_{e=1}^{N_{el}} \int_{\Omega^e} \tau \nabla \psi_i \cdot \sum_{j=1}^M (h_j \nabla \psi_j) d\Omega, \quad (25)$$

$$(\mathbf{G}_v \mathbf{h}_p)_i = \sum_{j=1}^M G_{v,ij} h_{p,j} = \sum_{e=1}^{N_{el}} \int_{\Omega^e} \tau \frac{\partial [Re\mathbf{u}^h \cdot \nabla \mathbf{u}^h - \nabla \cdot \mathbf{T}^h]}{\partial u_j} \cdot \sum_{j=1}^M (h_j \nabla \psi_j) d\Omega, \quad (26)$$

where summation over the number of pressure basis functions  $M$  has been moved inside the integral without loss of generality. Also, because  $\mathbf{G}_p$  is symmetric,  $\mathbf{G}_p^T \mathbf{h}_p = \mathbf{G}_p \mathbf{h}_p$ . We conclude that if

$$\sum_{j=1}^M (h_j \nabla \psi_j) = 0, \quad (27)$$

then  $\mathbf{J}^T \mathbf{h} = 0$ , which is the desired result.

We are only able to prove that Equation (27) holds for a given pressure basis type on a case by case basis. Note that the sum in Equation (27) is taken over all  $M$  pressure basis functions, whereas in Equation (16) the sum is over a subset  $M_h$  of the basis set. For any basis set in which  $M_h = M$ ,  $h_j$  must equal the same arbitrary constant for all  $j$ . Then  $h_j$  can be moved outside the sum, and Equation (16) applies. For quadrilateral (2D) and hexahedral (3D) elements these include constant discontinuous, continuous bilinear, continuous trilinear, continuous biquadrilateral, and continuous triquadrilateral basis functions. For triangular (2D) and tetrahedral (3D) elements these include linear-continuous basis functions. Linear-discontinuous basis functions provide an example in which  $M_h < M$ . In this case,  $h_j$  must equal the same arbitrary constant for all the constant members of the set, and zero otherwise. But  $\nabla \psi_j = 0$  for these members, so Equation (27) must hold.

Though we cannot prove Equation (27) in general, we suspect that it holds for all valid pressure basis function types used in conjunction with pressure-stabilized methods. Our basis for this statement is that any valid pressure basis must implicitly contain the hydrostatic null vector, which from Equation (22) requires that  $\mathbf{G}_p \mathbf{h}_p = \mathbf{0}$ , which would imply Equation (27).

It is easy to extend this analysis to the GLS case, in which Equation (22) is modified by the addition of terms to both upper blocks that arise from SUPG stabilization [5]. Modifications to the upper left block do not alter the conclusions. The additional terms that appear in the upper right block incorporate the gradient of pressure basis functions in a manner similar to Equation (26). Thus these terms do not alter the conclusions provided that Equation (27) is satisfied.

Likewise, it is a simple matter to incorporate time dependence to the analysis. In the GFEM, time dependent terms modify only the upper left block. In PSPG and GLS, additional terms also appear in the lower left block, but once again these terms do not alter the conclusions provided that Equation (27) is satisfied.

Brown and Walker [9] also prove that under the conditions for which GMRES converges to a least-squares solution without breakdown, the solution  $\mathbf{x}_m^{(k)}$  is unique.  $\mathbf{x}_m^{(k)}$  represents the solution update in Equation (7), which is added to the solution at the previous iteration, therefore, it is concluded that the hydrostatic pressure level is uniquely determined, and is set by the initial guess. We have verified this conclusion with numerical experiments in which the initial guess is shifted by an arbitrary constant, which results in a shift of the computed pressure field by exactly the same constant. It is easy to appreciate this result by noting that

Table III. GFEM-discretized 3D lid-driven cavity results (symbols explained in text)

Case	Formulation	$\int_{\Omega} \nabla \cdot \mathbf{u}^h d\Omega$	$ \int_{\Omega^e} \nabla \cdot \mathbf{u}^h d\Omega _{\max}$	$w_{\min}$	$w_{\max}$	$V_n$
1	Consistent singular	$3 \times 10^{-15}$	$2 \times 10^{-10}$	$-2.87 \times 10^{-2}$	$2.87 \times 10^{-2}$	–
2	Pressure datum	$3 \times 10^{-15}$	$6 \times 10^{-2}$	$-2.06 \times 10^{-2}$	$6.14 \times 10^{-2}$	–
3	Pressure datum	$2 \times 10^{-15}$	$2 \times 10^{-1}$	$-2.03 \times 10^{-2}$	$2.30 \times 10^{-1}$	–
4	Traction	$2 \times 10^{-2}$	$9 \times 10^{-6}$	$-2.08 \times 10^{-2}$	$1.40 \times 10^{-1}$	0.14

the addition of any amount of hydrostatic pressure to the initial guess does not alter the Krylov subspace, and therefore has no effect on Equation (19). The hydrostatic pressure level contained in the initial guess,  $\mathbf{y}^{(0)}$ , is simply carried along via Equation (7).

Ironically, it is when a pressure datum is set to remove the hydrostatic pressure mode that problems arise using GMRES. If the pressure datum differs much from the value that would otherwise be computed at that location (via the initial guess), then convergence of GMRES is greatly retarded. The results in Tables III and IV illustrate this situation.

Table III shows various measures of the computed solutions in four cases (all employing GFEM with a mixed interpolation; tests using GLS with equal-order interpolation on an unstructured mesh of tetrahedra produced similar results). Case 1 is the formulation in which no datum is set, leading as before to a consistent singular system. In Cases 2 and 3, a datum is set in the conventional manner by discarding an appropriate continuity residual and replacing it with a pressure value constraint. Different preconditioning methods were used in Cases 2 and 3. In Case 4, the node-freeing method discussed in Section 3.1 is employed in lieu of setting a pressure datum.

In Cases 1–3, the global divergence-free condition is satisfied to near machine precision, as indicated by the tabulated entries of  $\int_{\Omega} \nabla \cdot \mathbf{u}^h d\Omega$ . The linear-discontinuous pressure basis functions used here include a constant function, therefore, continuity should be also satisfied on each element. The results in Cases 2 and 3, however, show that the maximum elemental divergence,  $|\int_{\Omega^e} \nabla \cdot \mathbf{u}^h d\Omega|_{\max}$ , is quite large when a pressure datum is set. Significantly, this maximum occurs in the element in which the continuity residual has been discarded to set the pressure datum. In effect, a small area of large spurious divergence is balanced by a much larger area of slight divergence.

In Case 4, the results differ somewhat in that the global divergence-free condition is not satisfied. The cause is a leak at the boundary node at which the normal traction is imposed according to the node-freeing method. Another indication of this leak is the computed value

Table IV. Convergence of GFEM-discretized 3D lid-driven cavity results

Case	$L_{2,\text{GMRES}}$	$L_{2,\text{update}}$	$L_{\infty,\text{update}}$	$L_{2,\text{residual}}$	$L_{\infty,\text{residual}}$
1	$6 \times 10^{-10}$	$5 \times 10^{-11}$	$7 \times 10^{-10}$	$5 \times 10^{-12}$	$4 \times 10^{-10}$
2	$9 \times 10^{-6}$	$2 \times 10^{-5}$	$2 \times 10^{-4}$	$2 \times 10^{-7}$	$4 \times 10^{-6}$
3	$8 \times 10^{-5}$	$2 \times 10^{-7}$	$1 \times 10^{-7}$	$8 \times 10^{-7}$	$3 \times 10^{-5}$
4	$2 \times 10^{-5}$	$6 \times 10^{-10}$	$3 \times 10^{-9}$	$6 \times 10^{-8}$	$7 \times 10^{-7}$

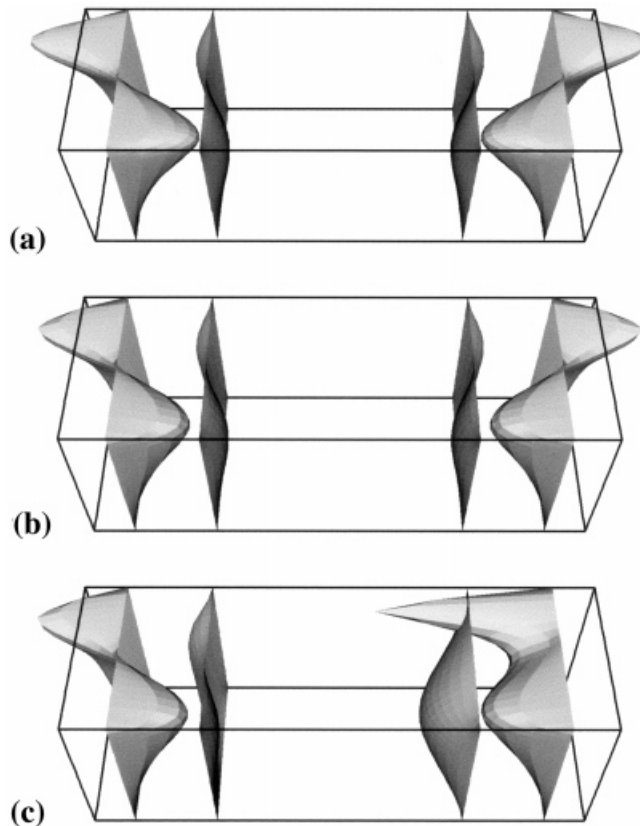


Figure 2. Transverse velocity profiles plotted at cuts symmetric about the midplane of the cavity, i.e.  $z = 0.25, 0.75, 2.25, 2.75$ , for the  $Re = 10$ , three-dimensional, lid-driven cavity solved via GFEM using Newton's method and GMRES. (a) Fine grid solution for Case 1, the consistent singular formulation. (b) Coarse grid solution for Case 1, the consistent singular formulation. (c) Coarse grid solution for Case 3, where a pressure datum is specified.

of  $V_n$  given in the table. The mass defect induced by this leak appears within the domain as a small divergence that is nearly equi-distributed among the elements. In fact, the condition  $\int_{\Omega} \nabla \cdot \mathbf{u}^h d\Omega = \int_{\Gamma} \mathbf{n} \cdot \mathbf{u}^h d\Gamma$  is satisfied to machine precision, but neither side of this equation is zero, due to the spurious leak at the boundary.

Another indication of a problem is seen by comparing the minimum and maximum values of the transverse velocity component,  $w$ . In the Case 1 computation, the flow is perfectly symmetric about the midplane of the domain and  $w_{\min} = -w_{\max}$ . Clearly, symmetric flow fields have not been obtained in the computations where a pressure datum has been set, i.e. Cases 2 and 3. Nor is a symmetric flow field obtained when the node-freeing method is employed in Case 4. These effects are further illustrated by the transverse velocity profiles plotted in Figure 2. The transverse velocity components are shown as 2D velocity profiles: vertical planes through the cavity are displaced by a number of units equal to 20 times the transverse velocity component. These profiles should be symmetric about the cavity midplane, as shown in Figure 2(a), in Case 1 computed with a fine mesh of  $15 \times 15 \times 30$  elements (202863 unknowns) to assess convergence of the solutions with respect to mesh refinement. Figure 2(b) shows the Case 1 computation on the coarser mesh used in the test calculations of this section. While somewhat less smooth than the fine mesh calculation, it is obviously still

symmetric about the midplane of the cavity. Figure 2(c) shows the results of the Case 3 computation; again, this flow is clearly unsymmetric. The flow in the  $x$ - $y$  plane is not strongly affected by the discrepancy in the relatively weak transverse flow component (see Figure 3). The inability to correctly predict flow symmetry is grave, however, because symmetry-breaking bifurcations are known to exist in the 3D lid-driven cavity [16].

These results make it clear that the solution is not fully converged in Cases 2 and 3 in the vicinity of the element in which the continuity residual has been discarded. Nor is the solution fully converged in Case 4 in the vicinity of the boundary node at which the normal traction is imposed. It is then relevant to inquire whether the various residual and update norms used to assess convergence give a clear indication of this condition. Table IV shows values of several norms, defined by Equations (19) and (9)–(12), respectively, in the four cases discussed above. In the Case 1 computation, all of the norms are very small, suggesting that convergence is achieved to a high degree. In Cases 2–4, the residual norms are several orders of magnitude larger, indicating that these solutions are less converged than that obtained in Case 1. Yet, the norms in these three cases still seem reasonably small, particularly the  $L_2$ -norms of the update and residual.

Understanding the behavior of the update norms,  $L_{2,\text{update}}$  and  $L_{\infty,\text{update}}$  requires a broader knowledge of the calculations. In Cases 2–4, the GMRES iteration stagnated, therefore, it was not possible to converge the solution to the linear system any better than shown in the table. Indeed, two different diagonal preconditioners were used in an attempt to converge the problem as much as possible (the type 2 and type 3 preconditioners described in Reference [11] were employed in Case 2 and 3, respectively). The solution update norms are small simply because GMRES has stagnated, not because the Newton iteration has converged. A small solution update demonstrates convergence of Newton's method, only if the linear system has been solved to a sufficient degree of precision, which evidently is not the case here. Instead, the Newton iteration has only reached a point where the solution of Equation (8) is orthogonal to the Krylov subspace.

The interpretation of the residual norms,  $L_{2,\text{residual}}$  and  $L_{\infty,\text{residual}}$ , in Cases 2–4 in Table IV again requires a deeper consideration. Unlike the solution update norms, the residual norms provide a measure of convergence that is independent of the accuracy of solution of the linear

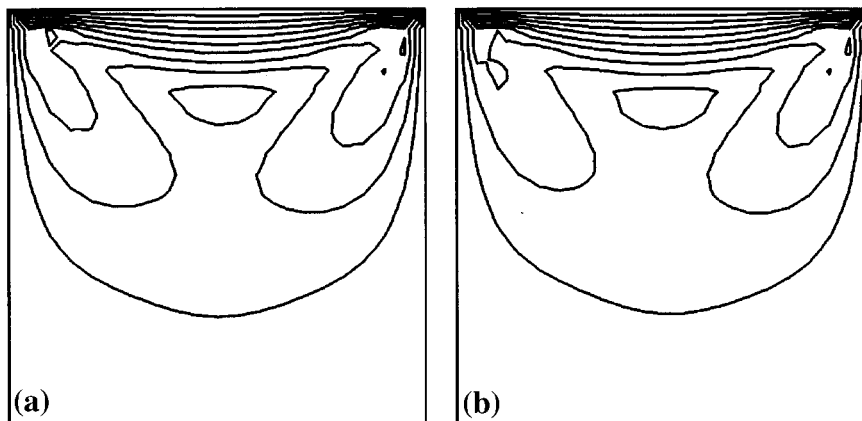


Figure 3. Speed contours in the  $x$ - $y$  plane at  $z = 2.75$  (contours range from 0 to 1 at intervals of 0.1) for the  $Re = 10$ , three-dimensional, lid-driven cavity solved via GFEM using Newton's method and GMRES. (a) Case 1, the consistent singular formulation. (b) Case 3, where a pressure datum is specified.

system (8). In this sense, the residual norms provide a more reliable indicator of convergence of Newton's method. However, the scale of the residuals is set by how well the discretized equations, in this case force balances, are satisfied. It is often more difficult to anticipate the magnitude of these forces than the magnitude of the unknowns in a given problem, because typically, the field variables can be reliably scaled to be  $\mathcal{O}(1)$  quantities. Consequently, it is often difficult to gauge the level of convergence by the absolute magnitude of the residuals. Case 3 is a good example of this outcome; while the  $L_{\infty, \text{residual}} = 3 \times 10^{-5}$  appears rather small, the computed solution still contains a significant error, as evidenced by the unsymmetric flow shown in Figure 2(c).

We do not have a rigorous explanation for why GMRES stalls without converging when a pressure datum is imposed. Numerical experiments in which the initial guess is shifted by an arbitrary constant provide some illumination, however. Over most of the domain the computed pressure is shifted by the same constant, similar to results described above in the consistent singular case. But the pressure basis coefficient at which a datum is set converges to the value of the imposed datum, whether or not this value matches the hydrostatic pressure level elsewhere. As a result, a pressure spike occurs in the immediate neighborhood of the element at which the pressure datum was set. It is this non-physical pressure spike that produces the unsymmetric flow artifact in Figure 2(c). We speculate that the difficulty arises from the inability of GMRES to construct a suitably rich Krylov projection subspace to represent a hydrostatic contribution to the pressure field. Such a contribution is required to shift the pressure field in accordance with the level set by the datum.

#### 4. CONCLUDING REMARKS

Several areas of concern have been identified when using modern FEM formulations for calculating enclosed, steady, incompressible flows. Under certain situations, an improper accommodation of the hydrostatic pressure can lead to inconsistencies or, even more importantly, significant error in computed velocity fields. Numerical examples of such effects were presented in this manuscript.

The first issue involves the use of pressure-stabilized formulations in conjunction with a direct solver. Removing the extra constraint of the hydrostatic pressure mode is generally desirable; however, the conventional approach of discarding one of the residuals in order to set a pressure basis coefficient violates the consistency and completeness of the underlying formulation. While our test calculations found that this violation did not lead to severe consequences, a more consistent method of accommodating the hydrostatic pressure mode is to apply a boundary traction condition, as described in Section 3.1. The boundary traction idea is not totally new [2]; however, this approach takes on added value in the context of pressure-stabilized formulations.

The second issue discussed in this manuscript is potentially more important, because it can lead to significant error in computing velocity fields. This issue arises when solving the consistent singular discrete system using an iterative solver. The results of Section 3.2 demonstrated that the setting of a pressure datum can slow or even stop the convergence of a GMRES-based iterative solver. While we have not presented rigorous arguments to explain this effect, we believe that it arises from the inability of GMRES to construct a suitably rich Krylov projection subspace, especially if the pressure field contained within the initial solution vector is inconsistent with the desired datum. This behavior is made even more dangerous by the possible misinterpretation of vector norms commonly used to judge convergence. If the

iterative method stagnates, the interpretation of the solution update norm becomes unreliable, i.e. a small update vector does not necessarily imply convergence. Alternatively, monitoring of the residuals norm can also be unreliable due to scaling uncertainty. In very large problems, such as those encountered in the calculation of three-dimensional flows, the  $L_2$ -norm can effectively mask local non-convergence by averaging over many degrees of freedom. Due to these issues, we advocate the solution of the consistent singular problem when iterative methods are employed. It is shown that GMRES converges in such cases, whether using the conventional GFEM, or pressure-stabilized formulations such as GLS and PSPG. This strategy results in a pressure datum set implicitly by the method, rather than explicitly by the user.

The phenomenon described above is not limited to the lid-driven cavity, nor to the classical GFEM formulation. We have observed similar results in a GLS discretized lid-driven cavity, as well as the problem of concentric rotating cylinders (for which an exact solution is available), and several other problems (see, e.g. the solution crystal growth hydrodynamical calculations of Yeckel *et al.* [19]). Nor does setting a boundary traction in the manner described in Section 3.1 improve the situation. Thus, it can be concluded that the negative effect of setting a pressure datum or boundary traction is a general concern when using GMRES, and most likely, also when using other projection-based iterative solvers.

#### ACKNOWLEDGMENTS

This work was supported in part by the National Science Foundation, under grant numbers DMR-9058386 and CTS-9218842, and the Army High Performance Computing Research Center under the auspices of the Department of the Army, Army Research Laboratory co-operative agreement DAAH04-95-2-0003/contract DAAH04-95-C-0008, the content of which does not necessarily reflect the position or policy of the government, and no official endorsement should be inferred. Additional computer resources were provided in part by the Minnesota Supercomputer Institute. We also gratefully acknowledge T.E. Tezduyar and his group at the University of Minnesota for use of their mesh generation software developed through the AHPCRC research program, V.F. de Almeida and Y.-I. Kwon for useful discussions related to this work, and an anonymous reviewer whose helpful comments and suggestions significantly improved the paper.

#### REFERENCES

1. R.L. Sani, P.M. Gresho, R.L. Lee and D.F. Griffiths, 'The cause and cure (?) of the spurious pressures generated by certain FEM solutions of the incompressible Navier–Stokes equations: Part 1', *Int. J. Numer. Methods Fluids*, **1**, 17–43 (1981).
2. R.L. Sani, P.M. Gresho, R.L. Lee, D.F. Griffiths and M.S. Engelman, 'The cause and cure (!) of the spurious pressures generated by certain FEM solutions of the incompressible Navier–Stokes equations: Part 2', *Int. J. Numer. Methods Fluids*, **1**, 171–204 (1981).
3. M.S. Engelman, R.L. Sani and P.M. Gresho, 'The implementation of normal and/or tangential boundary conditions in finite element codes for incompressible fluid flow', *Int. J. Numer. Methods Fluids*, **2**, 225–238 (1982).
4. T.E. Tezduyar, S. Mittal, S.E. Ray and R. Shih, 'Incompressible flow computations with stabilized bilinear and linear equal-order-interpolation velocity–pressure elements', *Comput. Methods Appl. Mech. Eng.*, **95**, 221–242 (1992).
5. T.E. Tezduyar, 'Stabilized finite element formulations for incompressible flow computations', in J.W. Hutchinson and T.Y. Wu (eds.), *Advances in Applied Mechanics*, Academic Press, New York, 1992, pp. 1–44.
6. T.J.R. Hughes, L.P. Franca and G.M. Hulbert, 'A new finite element formulation for computational fluid dynamics: VIII. The Galerkin/least-squares method for advective diffusive equations', *Comput. Methods Appl. Mech. Eng.*, **73**, 173–189 (1989).

7. Y. Saad and M.H. Schultz, 'GMRES: A generalized minimal algorithm for solving nonsymmetric linear systems', *SIAM J. Sci. Stat. Comput.*, **7**, 856–869 (1986).
8. Y. Saad, *Iterative Methods for Sparse Linear Systems*, PWS Publishing, Boston, 1996.
9. P.N. Brown and H.F. Walker, 'GMRES on (nearly) singular systems', *SIAM J. Matrix Anal. Appl.*, **18**, 37–51 (1997).
10. T.J.R. Hughes, *The Finite Element Method*, Prentice Hall, Englewood Cliffs, NJ, 1987.
11. A. Yeckel and J.J. Derby, 'Parallel computation of incompressible flows in materials processing: Numerical experiments in diagonal preconditioning', *Parallel Comput.*, **23**, 1379–1400 (1997).
12. A.G. Salinger, Q. Xiao, Y. Zhou and J.J. Derby, 'Massively parallel finite element computations of three-dimensional, time-dependent, incompressible flows in materials processing systems', *Comput. Methods Appl. Mech. Eng.*, **119**, 139–156 (1994).
13. P.M. Gresho, 'On pressure boundary conditions for the incompressible Navier–Stokes equations', in R.H. Gallagher, R. Glowinski, P.M. Gresho, J.T. Oden and O.C. Zienkiewicz (eds.), *Finite Elements in Fluids*, Wiley, New York, 1987, pp. 123–157.
14. P.M. Gresho, 'Incompressible fluid dynamics: some fundamental formulation issues', *Annu. Rev. Fluid Mech.*, **23**, 413–453 (1982).
15. C.J. Freitas and R.L. Street, 'Non-linear transient phenomena in a complex recirculating flow: a numerical investigation', *Int. J. Numer. Methods Fluids*, **8**, 769–802 (1988).
16. C.K. Aidun, N.G. Triantafillopoulos and J.D. Benson, 'Global stability of a lid-driven cavity with throughflow: Flow visualization studies', *Phys. Fluids A*, **3**, 2081–2091 (1991).
17. T.P. Chiang, R.R. Hwang and W.H. Sheu, 'Finite volume analysis of spiral motion in a rectangular lid-driven cavity', *Int. J. Numer. Methods Fluids*, **23**, 325–346 (1996).
18. P.M. Gresho, R.L. Lee and R.L. Sani, 'On the time-dependent solution of the incompressible Navier–Stokes equations in two and three dimensions', in R.H. Gallagher, R. Glowinski, P.M. Gresho, J.T. Oden and O.C. Zienkiewicz (eds.), Pineridge Press, Swansea, UK, 1980, pp. 27–81.
19. A. Yeckel, Y.-I. Kwon and J.J. Derby, 'Parallel computation of three-dimensional, time-dependent hydrodynamics during solution crystal growth', in S.N. Atluri and G. Yagawa (eds.), *Advances in Computational Engineering Science*, Tech. Science Press, Forsyth, Georgia, 1997, pp. 794–799.